Heliyon 10 (2024) e29285

Contents lists available at ScienceDirect

Heliyon

journal homepage: www.cell.com/heliyon

Research article

EEPD1 is identified as a predictor of prognosis and immune microenvironment through pan-cancer analysis and related to progression of colorectal cancer

Yang Guo [a,1], Shujin Li [b,1], Zhan Shi [a,1], Bingchen Chen [a], Ziang Wan [a], Peng Yu [a], Boan Zheng [a], Wenjing Gong [a], Rui Chai [a], Shiliang Tu [a,**], Hang Yuan [a,*]

[a] General Surgery, Cancer Center, Department of Colorectal Surgery, Zhejiang Provincial People's Hospital (Affiliated People's Hospital, Hangzhou Medical College) , Hangzhou, Zhejiang, 310014, PR China
[b] The Second Clinical Medical College, Zhejiang Chinese Medical University, Hangzhou, Zhejiang, 310053, PR China

ARTICLE INFO

Keywords:
EEPD1
CRC
Cell proliferation
Cell migration
Immune infiltration

ABSTRACT

Background: EEPD1 is vital in homologous recombination, while its role in cancer remains unclear.
Methods: We performed multiple pan-cancer analyses of EEPD1 with bioinformatics methods, such as gene expression, gene alterations, Prognosis and enrichment analysis, tumor microenvironment, immune cell infiltration, TMB, MSI, immunotherapy, co-expression of genes, and drug resistance. Finally, RT-qPCR, EdU, and transwell assays helped investigate the impact of EEPD1 on CRC cells.
Results: EEPD1 was dysregulated and correlated with bad prognosis in several cancers. GSVA and GSEA revealed that EEPD1 was primarily associated with the "WNT_BETA_CATENIN_SIGNALING," "ribonucleoprotein complex biogenesis," "Ribosome," and "rRNA processing." The infiltration of $CD8^+$ T cells, MAIT cells, iTreg cells, NK cells, Tc cells, Tex cells, Tfh cells, and Th1 cells were negatively correlated with EEPD1 expression. Additionally, EEPD1 is significantly associated with TMB and MSI in COAD, while enhanced CRC cell proliferation and migration.
Conclusions: EEPD1 was dysregulated in human cancers and correlated with various cancer patient prognoses. The dysregulated EEPD1 expression can affect tumor-infiltrating immune cells and immunotherapy response. Therefore, EEPD1 could act as an oncogene associated with immune cell infiltration in CRC.

Abbreviations: CRC, Colorectal cancer; ATR, ATM-and Rad3-Related; EEPD1, Endonuclease/exonuclease/phosphatase family domain containing 1; TCGA, The Cancer Genome Atlas; GTEx, Genotype-Tissue Expression; UCSC, University of California, Santa Cruz; COAD, colon adenocarcinoma; GSEA, Gene Set Enrichment Analysis; GSVA, Gene Set Variation Analysis; TME, Tumor Microenvironment; MHC, Histocompatibility complex; EMT, Epithelial-Mesenchymal Transition; MMR, Mismatch repair; GDSC, Genomics of Drug Sensitivity in Cancer; TMB, Tumor mutational burden; MSI, Microsatellite Instability; APC, Adenomatous polyposis coli.

* Corresponding author.General Surgery, Cancer Center, Department of Colorectal Surgery, Zhejiang Provincial People's Hospital, People's Hospital of Hangzhou Medical College, Hangzhou, Zhejiang, 310014, PR China.
** Corresponding author. General Surgery, Cancer Center, Department of Colorectal Surgery, Zhejiang Provincial People's Hospital, People's Hospital of Hangzhou Medical College, Hangzhou, Zhejiang, 310014, PR China.
E-mail addresses: tushiliang@126.com (S. Tu), 3011831022@163.com (H. Yuan).
[1] These authors contributed equally to this work as co-first authors.

https://doi.org/10.1016/j.heliyon.2024.e29285
Received 16 August 2023; Received in revised form 3 April 2024; Accepted 4 April 2024
Available online 4 April 2024

1. Introduction

Globally, cancer is a severe health problem. The CA: A Cancer Journal for Clinicians reveals that, in 2020, there were 19.3 million incidences and nearly 10 million mortalities associated with cancer worldwide [1]. Colorectal cancer (CRC) is a significant digestive system cancer. In 2020, CRC accounted for 10% of new cancer cases and 9.4% of cancer deaths [1]. Early colorectal cancer can be cured using surgical resection, adjuvant radiotherapy, and chemotherapy. However, metastatic CRC is complicated to resect directly using surgery. Currently, systemic treatments such as cytotoxic chemotherapy and immunotherapy are mainly used. They depict 1-year and 5-year survival rates of about 70%–75% and below 20%, respectively [2]. Therefore, the occurrence and developmental mechanism of CRC should be studied to identify appropriate therapeutic targets and improve the overall survival rate in advanced CRC.

DNA double-strand unties and creates a replication fork during replication. The replication fork process slows down or stagnates during exogenous or endogenous cellular DNA damage, a phenomenon called replication stress [3]. When the replication fork stagnates, an extensive range of single-stranded DNA extension [4] usually occurs, causing ATM-and Rad3-Related (ATR) kinases-mediated replication stress response [5]. This response suppresses cell cycle processes and provides DNA repair time [3]. Primarily, the stressed replication fork is repaired by homologous recombination (HR), which recombines homologous sequences between non-sister chromatids or within the same chromosome. The stagnated replication forks would create a free double-stranded DNA end structure. Then, 3′ single-stranded DNA would initiate HR through the 5′ end resection for DNA repair [6,7].

Endonuclease/exonuclease/phosphatase family domain containing 1 (EEPD1), first characterized in 2015, is a structure-specific nuclease with a vital role in rescuing stressed replication forks and HR [8]. According to Wu et al., EEPD1 can initiate HR by facilitating the 5 ′end resection, enabling the replication fork to resist replication stress and maintain genomic stability [9]. Additionally, EEPD1 can load DNA repair components onto broken replication forks [9]. Oncogenes induce replication stress through ROS, abnormal replication initiation, and hyper transcription [10]. The cancer cell DNA will replicate during damage, making cancer cells experience continuous replication stress [11]. EEPD1 provides DNA resistance to replication stress for better cell survival, indicating its vital role in the life cycle of tumors. Hromas et al. revealed that HR-deficient breast cancer cells exhibit synthetic lethality during RAD52 depletion, possibly mediated by EEPD1 [12]. However, with limited research on EEPD1, its role in cancer remains unclear.

2. Materials and methods

2.1. Data sources

The gene expression data for the tumor tissues were retrieved from The Cancer Genome Atlas (TCGA) database, while that of normal tissues was obtained from TCGA and Genotype-Tissue Expression (GTEx) databases maintained by the Xena (https://xena.ucsc.edu/) database of the University of California, Santa Cruz (UCSC).

2.2. EEPD1 pan-cancer alterations analysis

Gene alterations and their results were explored and visualized by the cBioportal (http://www.cbioportal.org) and its web tool, respectively.

2.3. Prognosis analysis

TCGA database provided the clinical survival data. The association between EEPD1 expression and cancer patient survival underwent univariate COX regression analysis using R packages "survival" and "forestplot." "Survminer" and "survival" packaged from R were used to perform the survival analysis using the Kaplan-Meier method. P value < 0.05 was considered statistically significant.

2.4. Enrichment analysis

We determined the correlation between EEPD1 and other genes using the Pearson method with the colon adenocarcinoma (COAD) data from TCGA. We selected 300 genes with the most significant positive correlation for Gene Set Enrichment Analysis (GSEA) using GO, KEGG, rectome databases, and the R package "clusterprofiler." In addition, the HALLMARK pathway dataset of the MsigDB database was utilized to determine the Gene Set Variation Analysis (GSVA) scores in CRC and analyze the association of EEPD1 expression with its scores.

2.5. Tumor microenvironment (TME) analysis

We calculated TumorPurity, Stromalcore, ImmuneScore, and ESTIMATEScore on the COAD gene expression data using R packages "ESTIMATE" for elucidating their association with EEPD1 levels. In addition, the CIBERSORT algorithm helped infer TME-related pathways to analyze their correlation with EEPD1.

2.6. Immune cell infiltration and immune-related genes

The correlation of gene expression was determined with each infiltration data from immune cells of Pan-cancer retrieved from the TIMER2 database (http://timer.comp-genomics.org/) through a heat map. (Red boxes indicate positive associations, green depict negative associations, and boxes with a cross indicate $p > 0.05$). Also, the Infiltration Score of each immune cell was determined using the CIBERSORT algorithm in the ImmuCellAI database (http://bioinfo.life.hust.edu.cn/ImmuCellAI#!/). Then the EEPD1 correlation with each immune cell Infiltration Score in CRC was evaluated and depicted as a line plot. For circle plots, we chose cells with a Pearson correlation coefficient >0.15 with EEPD1 to perform correlation circle mapping. Red and green depict positive and negative correlations, respectively, with a stronger correlation as the color darkens. Besides, Pearson correlation analysis was utilized for EEPD1 and immune-related gene expression. This included immune checkpoints, chemokines, chemokines receptors, immune activation genes, immunosuppressive genes, major histocompatibility complex (MHC) genes, Epithelial-Mesenchymal Transition (EMT) down, EMT up, pyroptosis, autophagy, TGF-β1 signaling, Wnt/β-catenin signaling, ferroptosis, and mismatch repair (MMR) genes. We plotted heat maps using the R package "ggplot2".

2.7. TMB and MSI and immunotherapy response

The mutation data of 33 tumors were obtained from TCGA cohort of the Genomics of Drug Sensitivity in Cancer (GDSC) database. The tumor mutational burden (TMB) was acquired by the ratio of the mutation sites with the total exon length. A previous study obtained data on Microsatellite Instability (MSI) [13]. The association of EEPD1 levels with tumor immunotherapy response and patient prognosis post-therapy was obtained using the "IMvigor210CoreBiologies" dataset and R package "IMvigor210CoreBiologies".

2.8. Drug resistance analysis

A correlation analysis was performed between EEPD1 and the IC50 of 192 drugs using the GDSC data and significant statistical consideration at $P < 0.05$.

2.9. Nomogram development and verification

EEPD1 expression was determined with mean values, and the samples whose expression was higher than the mean value were classified as the EEPD1 high expression group. Based on this group, univariate and cox multivariate survival analyses helped determine the independent prognostic factors of CRC. A nomogram was constructed using these independent prognostic factors, and its accuracy was evaluated using a calibration plot. ROC curve (receiver operating characteristic curve) helped determine the nomogram efficiency and clinical factors in foreseeing the survival time in CRC patients at 1 -, 3 -, and 5-years.

2.10. CRC specimens collection

Twenty-three tumor and normal tissue pairs were sampled from CRC patients undergoing surgical intervention at the Zhejiang Provincial People's Hospital. Then the tissues were in a refrigerator at - 80 °C. The clinicopathological characteristics of colon cancer patients were listed in Table s1.

2.11. Cell culture and transfection

Colon cancer cell lines (HCT116, HCT8 and RKO) and the normal colon cell line NCM460 were obtained from the Fuheng Biology. We cultured HCT116 and NCM460 cell lines in the DMEM medium (Biological Industries, Israel) using 10% fetal bovine serum (Biological Industries, Israel) and Penicillin-Streptomycin (100 mg/mL) (NCM Biotech, Suzhou, China). Moreover, HCT8 and RKO cell lines were cultured in the RPMI1640 medium (Biological Industries, Israel) using 10% fetal bovine serum (Biological Industries, Israel) and Penicillin-Streptomycin (100 mg/mL) (NCM Biotech, Suzhou, China). At 37 °C, we culture the cell lines using a 5% CO_2 incubator. EEPD1 stRNA, designed and produced by ribobio (Guangzhou, China), was used to knock down EEPD1 in CRC cells. Lipofectamine 3000 (ThermoFisher Scientific, Massachusetts, USA) was used to transfect stRNA into CRCs. The sequence of stRNA is as follows: st-h-EEPD1#1 GCCTGTAACTTCAGCAACA; st-h-EEPD1#2 GCCGAGTTCTACACTGAAA; st-h-EEPD1#3 GCATGACACTCCTGGAAAA.

2.12. Immunohistochemistry (IHC)

We separately took tumor tissue and adjacent tissue from the same patient. Tissue samples were fixed in 4% paraformaldehyde, embedded in paraffin, and sectioned. Tissue sections were incubated with EEPD1 primary (1:1000, OriGene, Wuxi, China) antibody overnight at 4 °C and followed by HRP-conjugated secondary antibody.

2.13. RT-qPCR

The RNA-Quick Purification Kit (ES Science, Shanghai, China) facilitated the total RNA extraction from cells and tissues. Then, they were reverse-transcribed into cDNA based on the protocol of PrimeScript RT Kit (Takara, Japan). We performed the RT-qPCR using the

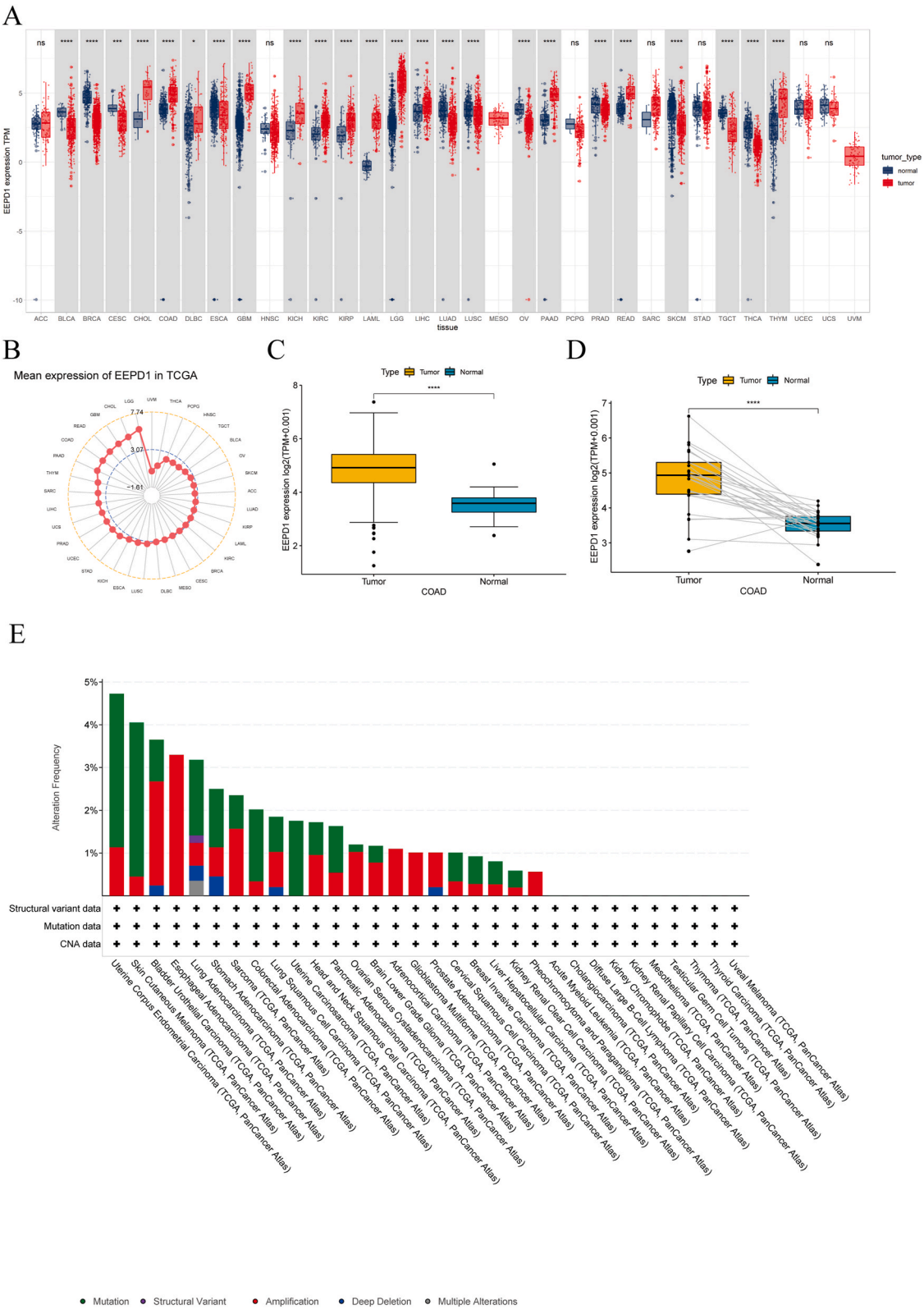

Fig. 1. EEPD1 Pan-Cancer expression and genetic alteration. (A) EEPD1 Pan-cancer differential expression according to TCGA and GTEx database. (B) Mean expression of EEPD1 in multiple cancers. (C) EEPD1 expression in COAD tumor tissues and normal tissues. (D) EPD1 expression in paired COAD tumor tissues and normal tissue. (E) EEPD1 pan-cancer genetic alterations in cBioportal database.

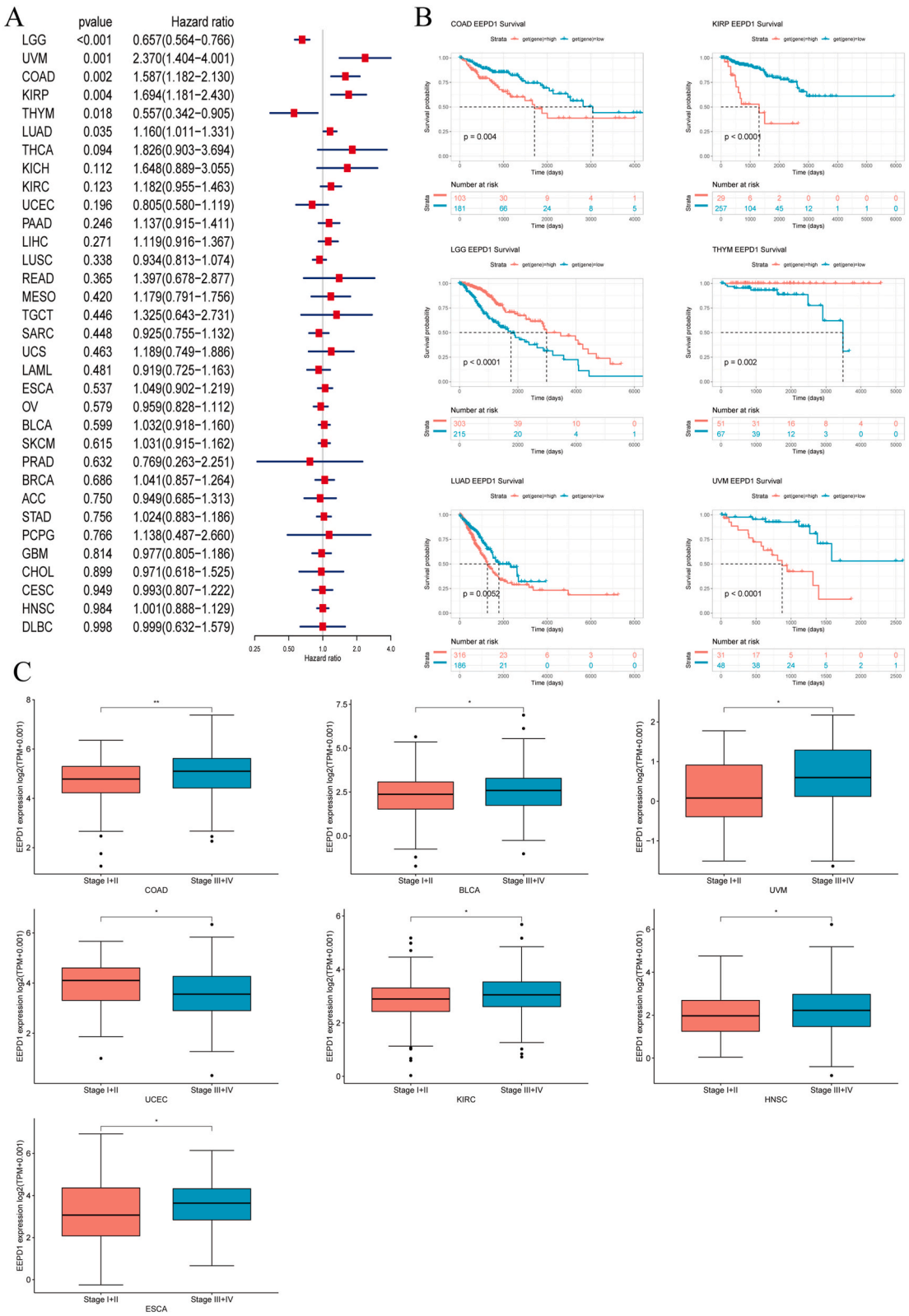

Fig. 2. Association between EEPD1 and prognosis and clinic phenotypes. (A) Forest plot based on the univariate COX regression analysis of EEPD1 and OS in 33 cancers (B) Kaplan-Meier analysis of association between EEPD1 and prognosis in cancers. (C) Association between EEPD1 and tumor stage in cancers.

qPCR SYBR Green Master Mix of Hieff UNICON® Universal Blue (Yeasen Biotechnology, Shanghai, China) and the ABI PRISM 7300 RT-PCR system (Applied Biosystems) on the synthesized cDNA. Triplicate reactions were performed using GAPDH as the reference. We determined the relative gene expression with the 2-ΔΔCt method. The sequence of EEPD1 primers is as follows:

h-EEPD1-144-F GAGGTTCAAGGTGGGAAGTC; h-EEPD1-144-R AGGGTTTCCTGTAGGGTCTGT.

2.14. Western blot

The cells were lysed using RIPA buffer (Boster Biological Technology Ltd., Wuhan, China). The protein concentration was determined based on the BCA protein assay kit (Boster). Proteins were separated by uusing PAGE Gel Quick Preparation Kit (Yeasen Biotechnology, Shanghai, China), and the separated proteins were electro-transferred onto a PVDF membrane (Millipore, Bedford, MA, USA). The membrane was probed with diluted primary antibodies followed by overnight incubation at 4 °C. The next day, the membrane was labeled with HRP-bound secondary antibody incubation (1:1000, Beyotime, Shanghai, China) and detected using an ECL system (Bio-Rad, California, USA). The resulting bands were scanned using the ChemiDocTM MP Imaging System (Bio-Rad, California, USA).

2.15. Cell proliferation experiments

Placing cell slides in a 24-well plate, adding 500ul of serum-free DMEM medium. Subsequently, transferring 10,000 well-growing cells into the wells with cell slides and incubating overnight in a cell culture incubator. Then, EdU experiments were performed based on the manufacturer's instructions from the In Vitro Kit of Cell-Light EdU Apollo567 (Ribobio, Guangzhou, China).and the results were observed with a Leica laser scanning confocal microscope (Leica, Munich, Germany). Three random fields were obtained to determine the positive rate.

2.16. Transwell investigations

Transwell experiments in specific chambers helped investigate migration (Corning, New York, USA). We resuspended 2×10^4 cells in 200ul of serum-free DMEM medium and placed them in the upper chamber. This was followed by adding 600ul of DMEM containing 10% FBS in the lower chamber. Then, they were kept in a 5% CO2 incubator at 37 °C for 48h. The cells migrating to the lower chamber were fixed with 4% paraformaldehyde and stained with 0.1% crystal violet. Finally, three random microscopic fields were used to count the number of migrated cells.

2.17. Statistical analysis

GraphPad Prism 8 was used to perform a *t*-test and at least three independent replicates were used as mean and standard deviation, with $P < 0.05$ indicating the significance level.

3. Results

3.1. EEPD1 pan-cancer expression

EEPD1 expression was first analyzed in multiple cancers using the tumor gene expression data downloaded from TCGA, with the maximum in LGG and minimum in UVM (Fig. 1B). EEPD1 expression in various cancers and normal tissues was also compared by combining TCGA and GTEx databases, which was higher in 12 cancers than in normal tissues. These cancers included cholangiocarcinoma (CHOL), COAD, Lymphoid Neoplasm Diffuse Large B-cell Lymphoma (DLBC), glioblastoma multiforme (GBM), Kidney Chromophobe (KICH), Kidney renal clear cell carcinoma (KIRC), kidney renal papillary cell carcinoma (KIRP), Acute Myeloid Leukemia (LAML), liver hepato-cellular carcinoma (LIHC), pancreatic adenocarcinoma (PAAD), rectum adenocarci-noma (READ) and Thymoma (THYM). However, there were lower EEPD1 levels in bladder urothelial carcinoma (BLCA), breast invasive carcinoma (BRCA), esophageal carcinoma (ESCA), cervical squamous cell carcinoma and endocervical adenocarcinoma (CESC), ovarian serous cystadenocarcinoma (OV), lung adenocarcinoma (LUAD), lung squamous cell carcinoma (LUSC), skin cutaneous melanoma (SCKM), prostate adeno-carcinoma (PRAD), testicular germ cell tumor (TGCT) and thyroid carcinoma (THCA) than in the normal tissues (Fig. 1A). CRC tissues indicated substantial statistical enhancement of EEPD1 levels (Fig. 1C,D), promoting tumor occurrence and development. Additionally, genetic alterations of EEPD1 in tumor samples from the cBi-oportal database were also analyzed. Fig. 1E represents the genetic alterations of EEPD1 in various tumors, including COAD, which were mainly "Mutation" and "Am-plification." However, the alteration frequency was <5%, depicting the relatively con-served sequence of EEPD1 (Fig. 1E). Therefore, EEPD1 was dysregulated in pan-cancer with a low genetic alteration frequency.

3.2. Correlation between EEPD1 and clinical phenotypes and prognosis of cancer patients

A univariate COX regression analysis of EEPD1 in 33 cancers helped determine the effect of EEPD1 on cancer patient prognosis. Therefore, the expression level of EEPD1 was associated with OS in patients with lower-grade glioma (LGG) within the brain, Uveal Melanoma (UVM), COAD, KIRP, THYM, and LUAD (Fig. 2A). EEPD1 was a high-risk factor in UVM, COAD, KIRP, and LUAD, while it

was low-risk in LGG and THYM (Fig. 2A). Moreover, Kaplan-Meier methods established the survival analyses in these six cancers. Increased EEPD1 levels in patients did not have a longer survival time than those with low EEPD1 levels in UVM, COAD, KIRP, and LUAD. In contrast, patients having high EEPD1 expression depicted a better prognosis than in LGG and THYM due to low levels (Fig. 2B). The pan-cancer tumor stage analysis indicated that EEPD1 expression was higher in advanced tumors in COAD, BLCA, UVM, KIRC, neck squamous cell carcinoma (HNSC), and ESCA, which was lower in advanced tumors in UCEC (Fig. 2C). Thus, EEPD1 was associated with the clinical phenotype and overall prognosis of cancer patients.

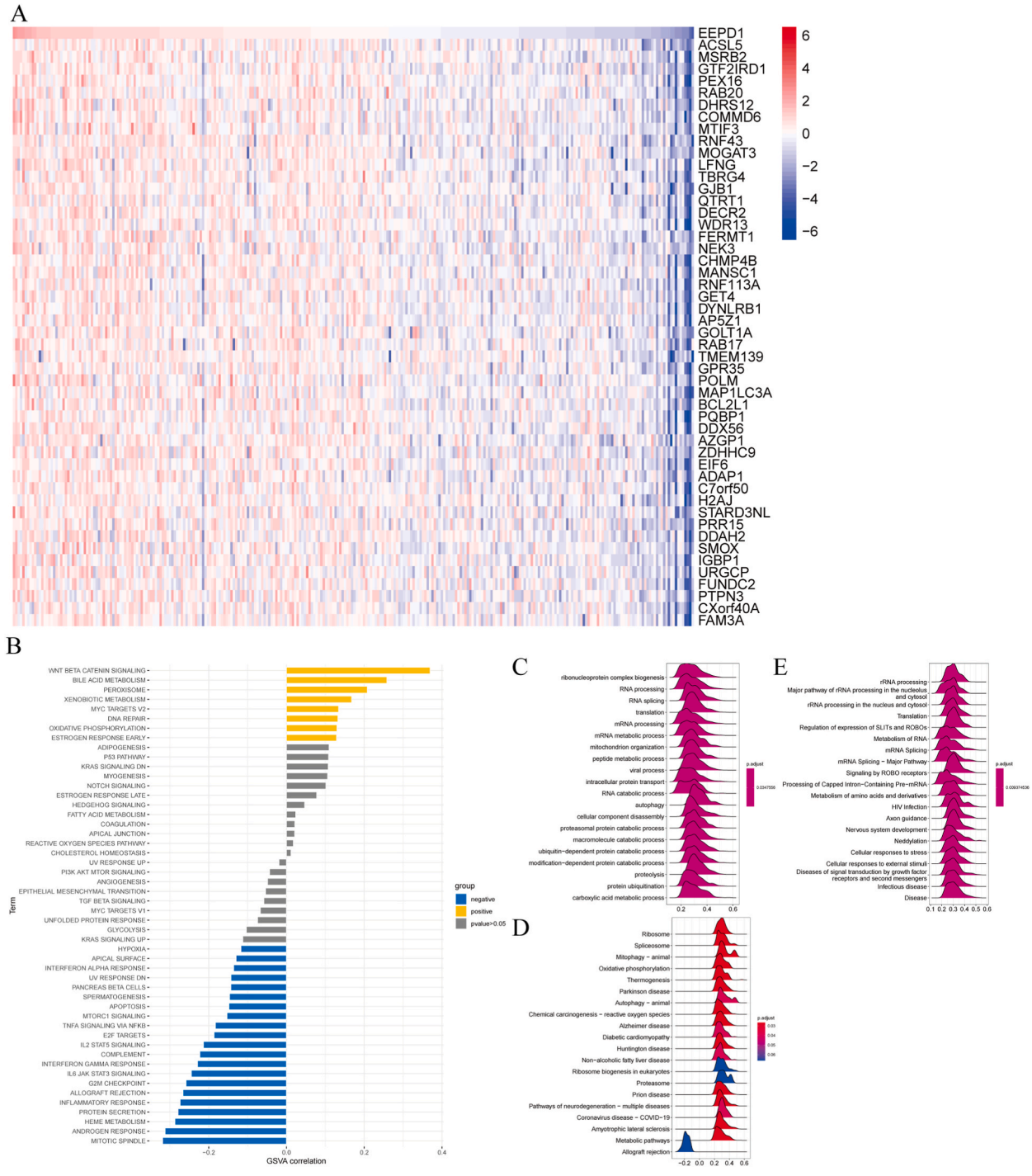

Fig. 3. Enrichment analysis of EEPD1 in colorectal cancer. (A) correlation analysis of EEPD1 in colorectal cancer. (B) GEVA of EEPD1 in colorectal cancer. (C–E) GSEA of EEPD1 based on GO, KEGG pathways and Reactome pathways.

3.3. GSVA and GSEA

EEPD1 was highly expressed in CRC patients with poor survival. We conducted a correlation analysis between EEPD1 and other genes to explore its biological function in CRC. Then, the best 50 genes showing significant positive association are depicted in Fig. 3A. Then, the 300 best positively correlated genes with EEPD1 were selected, and a Gene Set with EEPD1 was formed. A GSVA score was performed on all tumors to investigate the functional mechanism of EEPD1. The result indicated that EEPD1 is primarily associated with the WNT_BETA_CATENIN_SIGNALING, BILE_ACID_METABOLISM, and PEROXISOME (Fig. 3B). GSEA was performed ac-cording to GO, KEGG, and Reactome databases. GO analysis showed involvement in "ribonucleoprotein complex biogenesis," "RNA processing," and "RNA splicing" (Fig. 3C). KEGG genes were primarily enhanced in the "Ribosome," "Spliceosome," and "Mi-tophagy-animal" pathways (Fig. 3D). These genes were primarily enriched in "rRNA processing," "Major pathway of rRNA processing in the nucleolus and cytosol," and "rRNA processing in the nucleus and cytosol" based on Reactome database analysis (Fig. 3E).

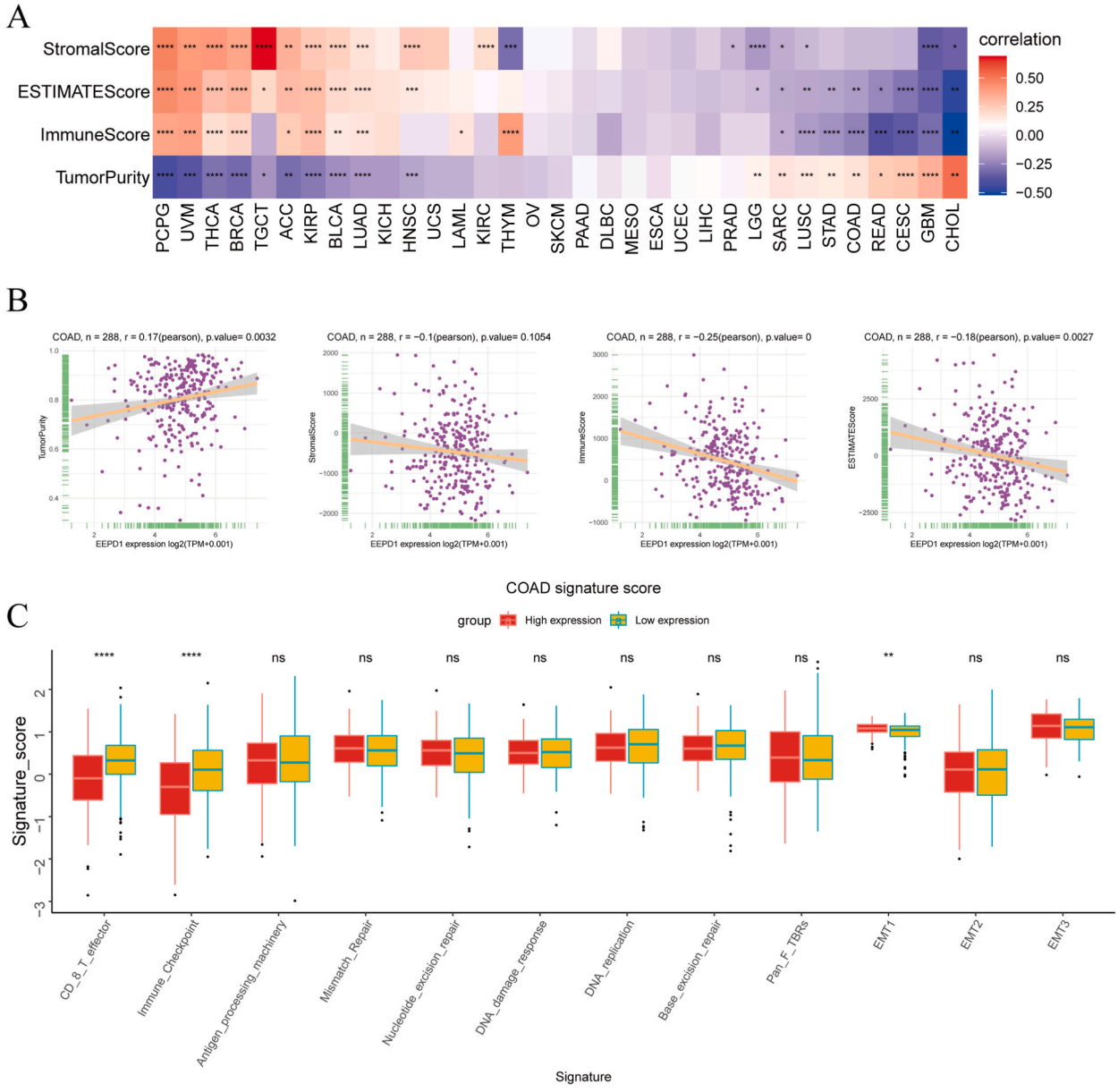

Fig. 4. TME analysis of EEPD1. (A) ESTIMATE analysis of EEPD1 in caners. (B) ESTIMATE analysis of EEPD1 in CRC. (C) The correlation between the expression level of EEPD1 and TME in COAD.

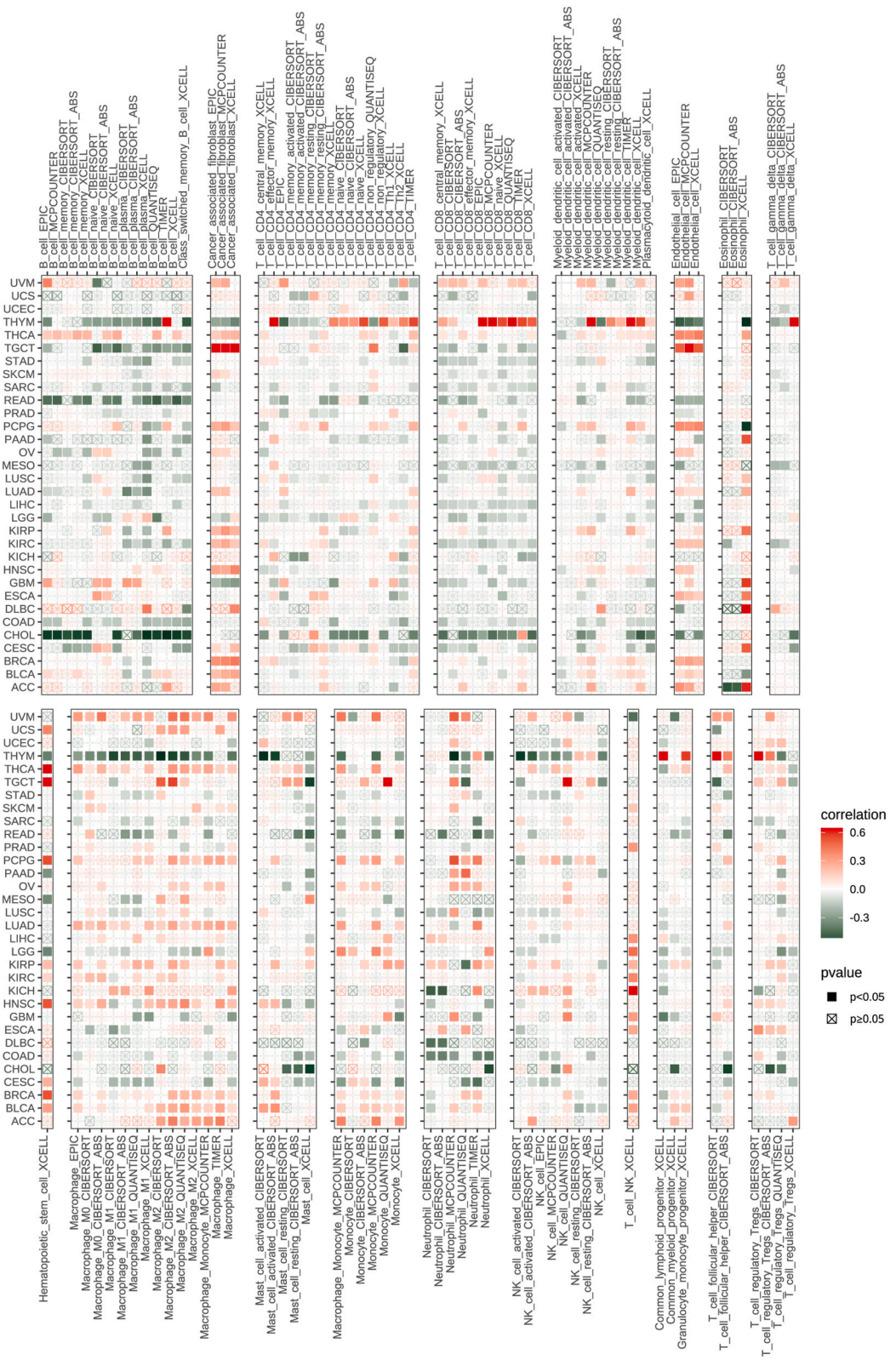

Fig. 5. The correlation between the expression of EEPD1 and pan-cancer immune cell infiltration based on TIMER2 (Red boxes represent positive associations, green negative associations, and boxes with a cross indicate $p > 0.05$). (For interpretation of the references to color in this figure legend, the reader is referred to the Web version of this article.)

3.4. EEPD1 and tumor microenvironment

Emerging evidence suggests that TME is closely associated with tumor develop-ment and metastasis [14]. This affects chemotherapy and immunotherapy and patient outcomes [15–17]. Therefore, the Tumor Purity, Stromal, Immune, and ESTIMATE Scores for each tumor were determined using the ESTIMATE program (Fig. 4A). A negative association was seen between expression and Immune Score in COAD, which was significant (Fig. 4B). Moreover, EEPD1 was also negatively associated with Immune Scores in CHOL, GBM, CESC, READ, STAD, LUSC, and SARC. In contrast, EEPD1 showed a positive association in PCPG, UVM, THCA, BRCA, ACC, KIRP, BLCA, LUAD, LAML, and THYM with Immune Scores (Fig. 4A). Afterward, EEPD1 and TME levels and their association were further analyzed in COAD, indicating a signifi-cant correlation with CD 8 T effector, Immune Checkpoint, and EMT1 (Fig. 4C). Therefore, the

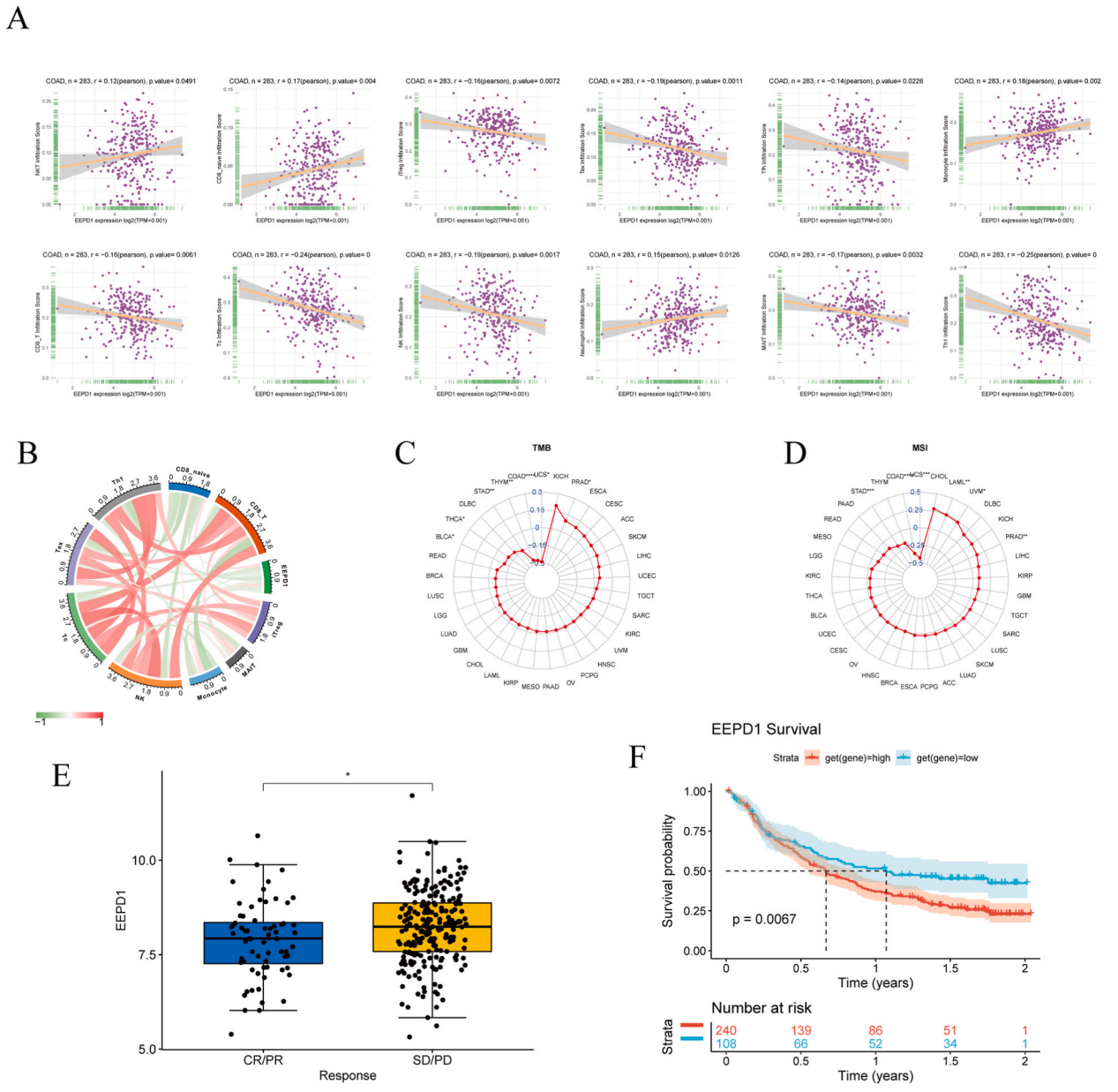

Fig. 6. (A)The correlation between EEPD1 expression and immune cell infiltration in colorectal cancer. (B)Circle plot of the correlation between EEPD1 expression and immune cell infiltration in colorectal cancer. cells with pearson correlation coefficient >0.15 with EEPD1 were selected for correlation circle mapping. Red represents positive correlation, green represents negative correlation, and the darker the color, the stronger the correlation. (C)The correlation between EEPD1 expression and TMB. (D) The correlation between EEPD1 expression and MSI. (E) The correlation between EEPD1 expression and tumor response to PD-L1 inhibitor. (F) Kaplan-Meier analysis of association between EEPD1 and prognosis in PD-L1 treated patients. (For interpretation of the references to color in this figure legend, the reader is referred to the Web version of this article.)

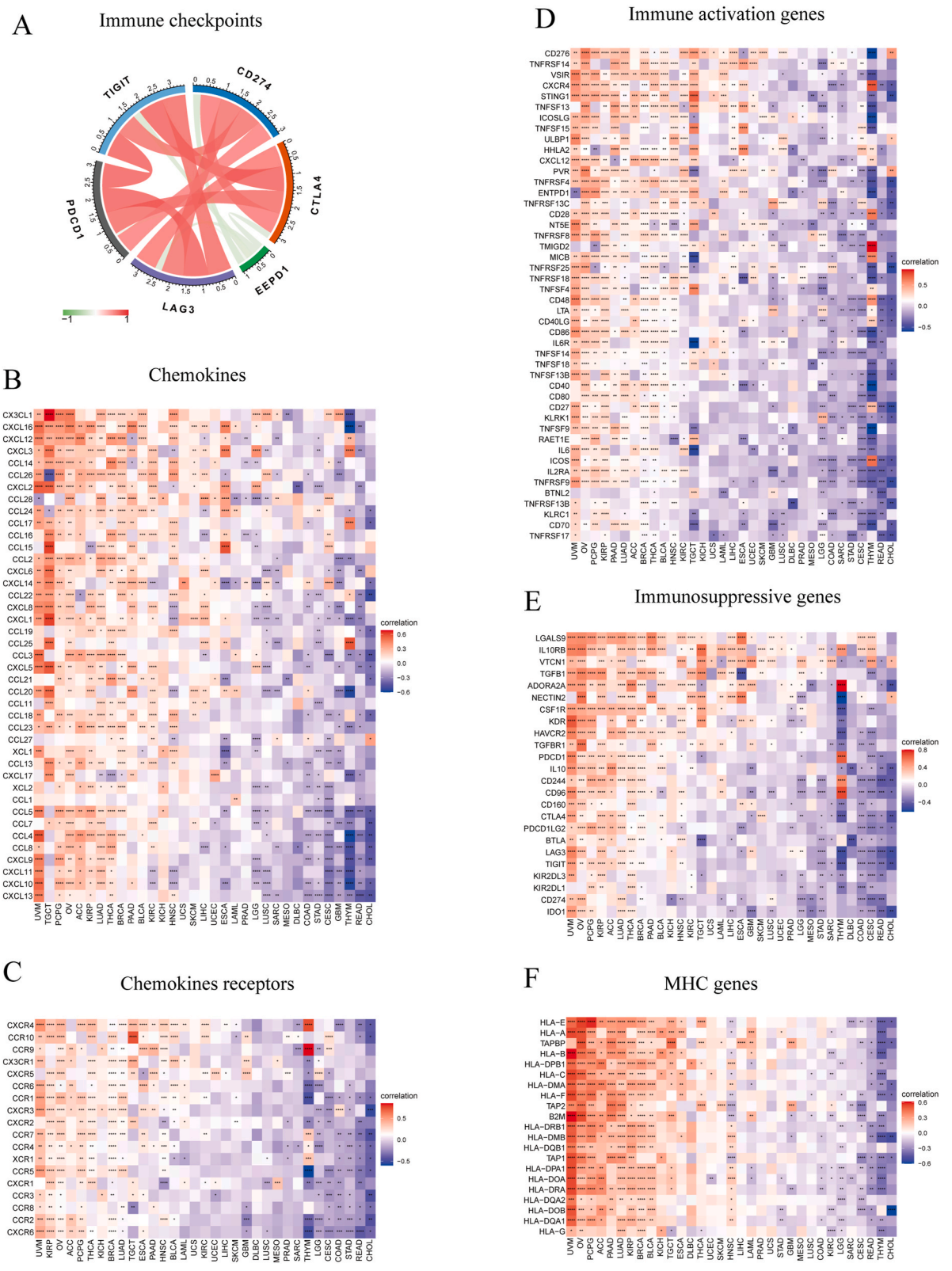

Fig. 7. The gene co-expression analysis of EEPD1 and (A) immune checkpoints, (B) chemokines, (C) chemokines receptors, (D) immune activation genes, (E) immunosuppressive genes, (F) MHC genes.

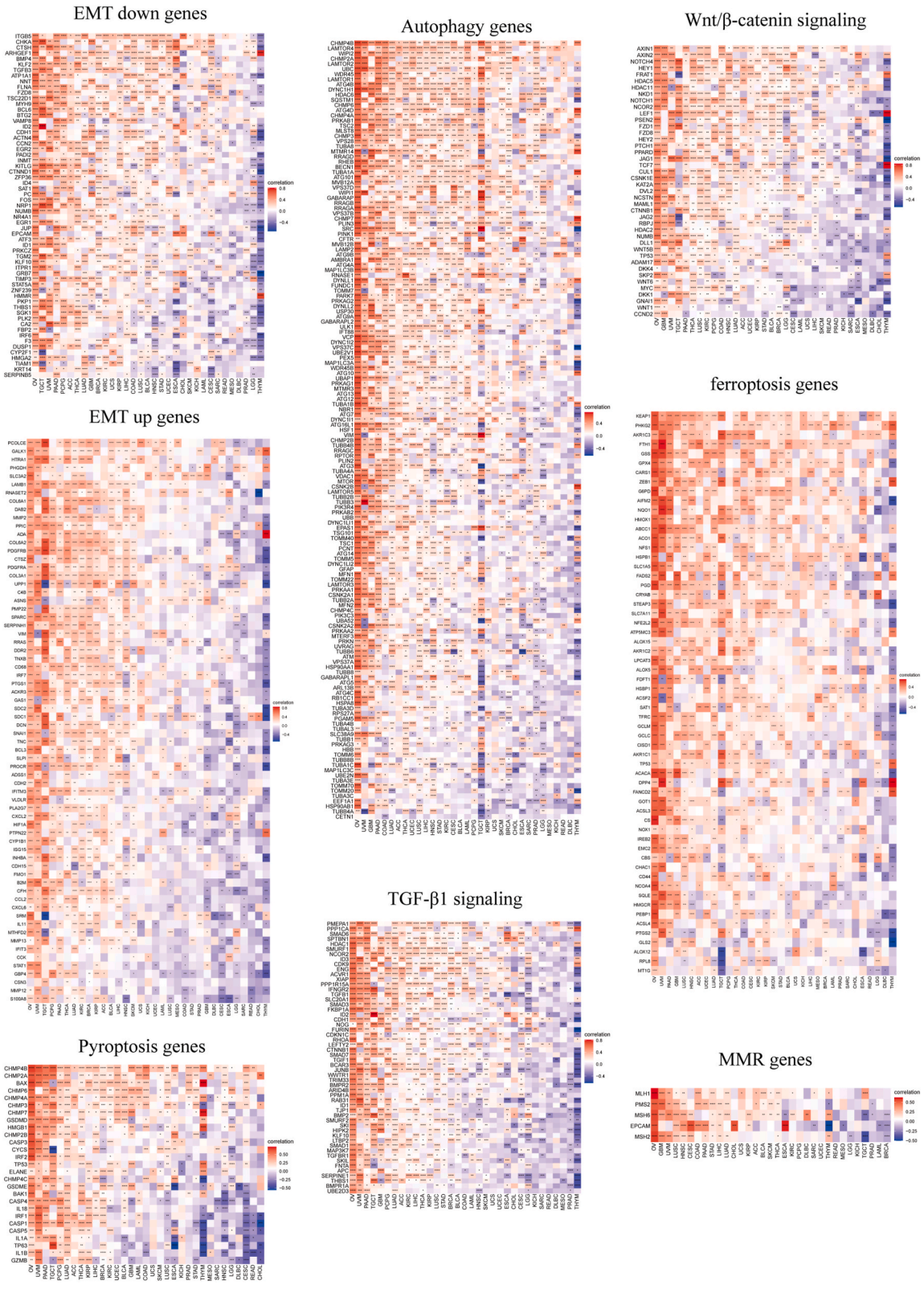

Fig. 8. The gene co-expression analysis of EEPD1 and (A) EMT down, (B) EMT up, (C) pyroptosis, (D) autophagy, (E) TGF-β1 signaling, (F) Wnt/β-catenin signaling, (G) ferroptosis, (H) MMR genes.

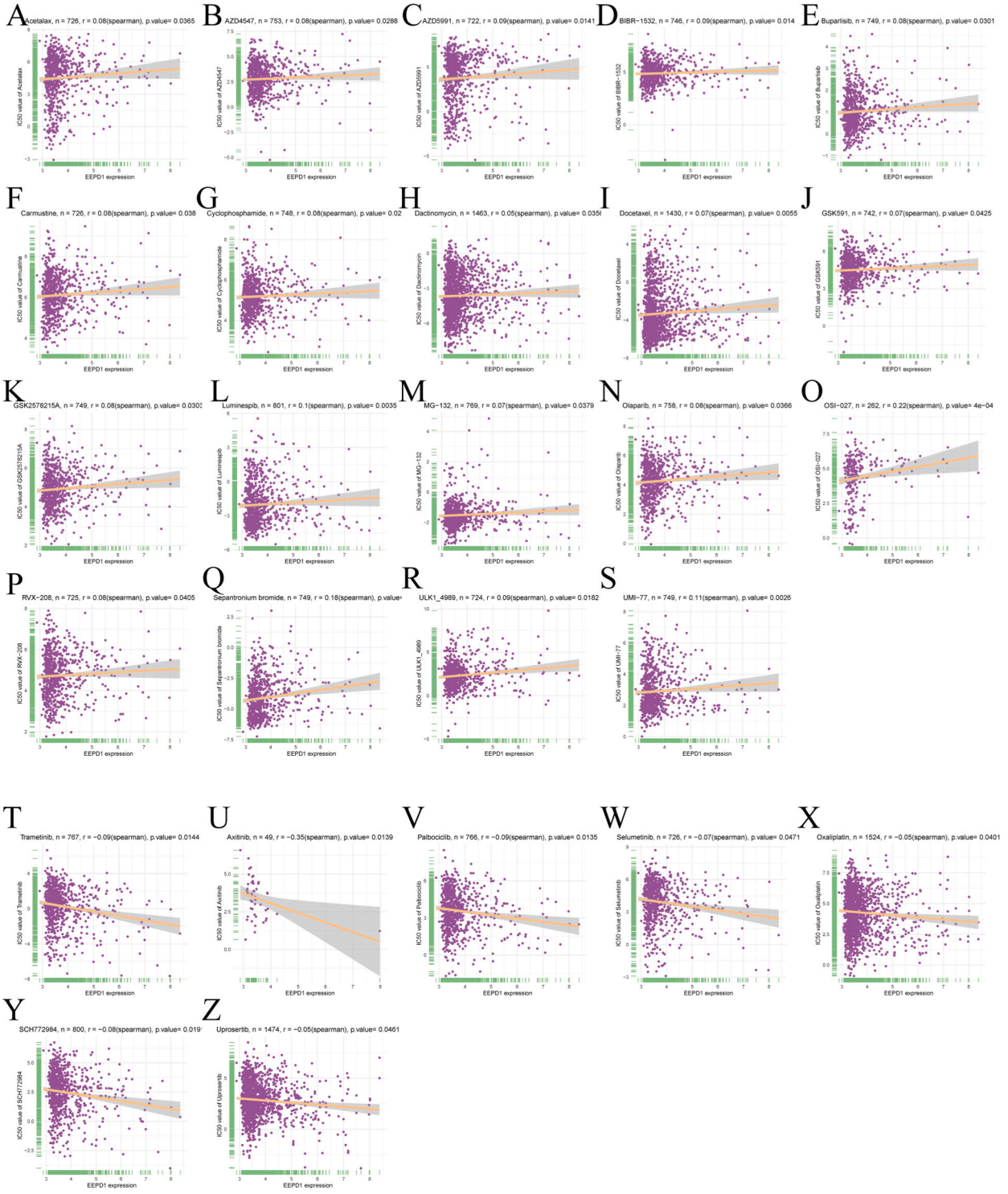

Fig. 9. The correlation between EEPD1 expression and IC50 of multiple drugs. (A–S) The EEPD1 expression is positive with IC50 of drugs. (T–Z) The EEPD1 expression is negative with IC50 of drugs.

expression of EEPD1 affects TME in various cancers, including CRC.

3.5. EEPD1 and immune cell infiltration

We explored the Pan-cancer immune infiltration data from the TIMER2 database to calculate the correlation with a heat map. (Red boxes indicate positive associations, green depict negative associations, and boxes with a cross represent $p > 0.05$) (Fig. 5). EEPD1

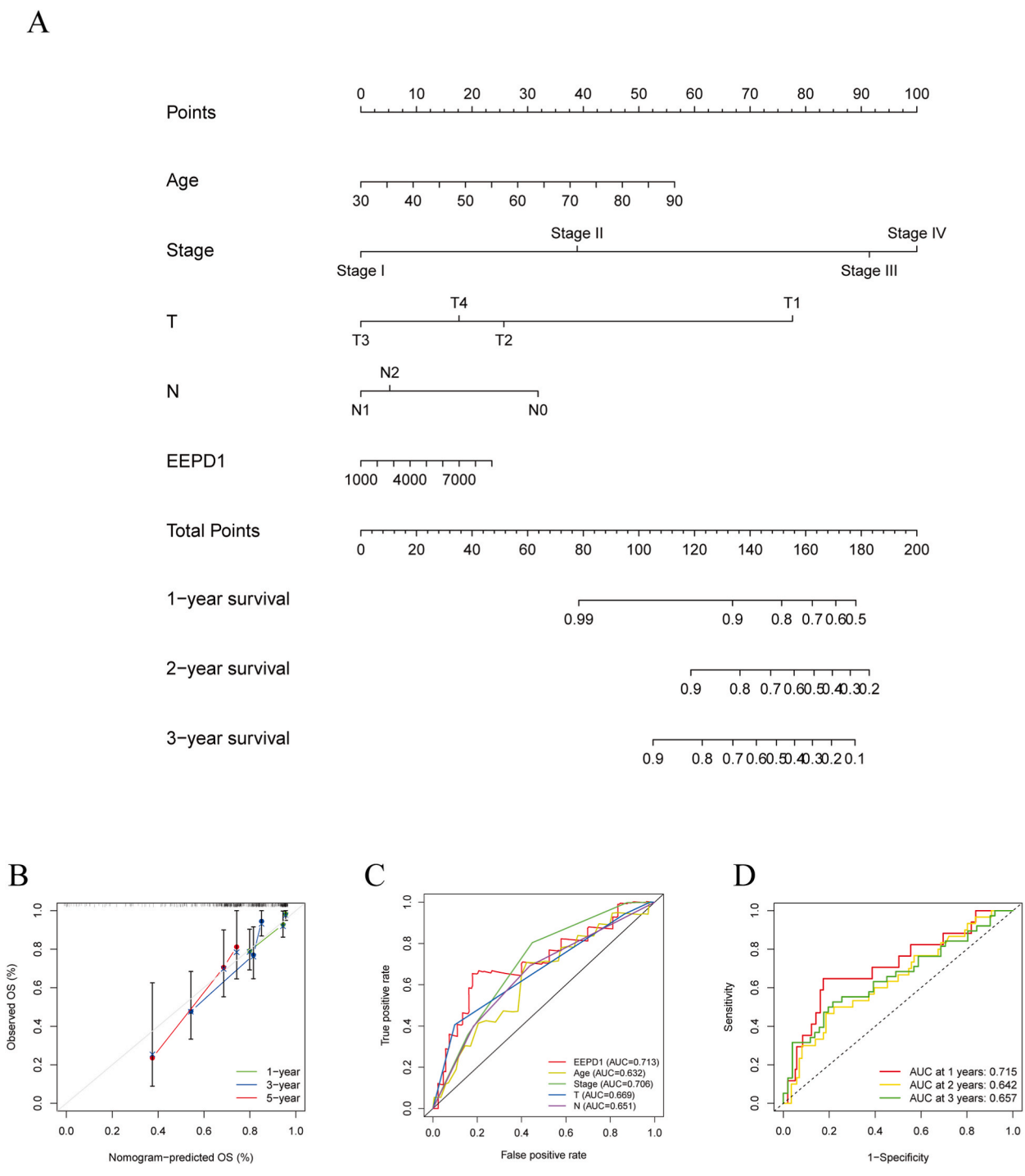

Fig. 10. (A)The nomogram to predict OS of CRC patients. (B) Calibration plot for the nomogram. (C) ROC curve for EEPD1 and other clinical parameters. (D) ROC curve for nomogram.

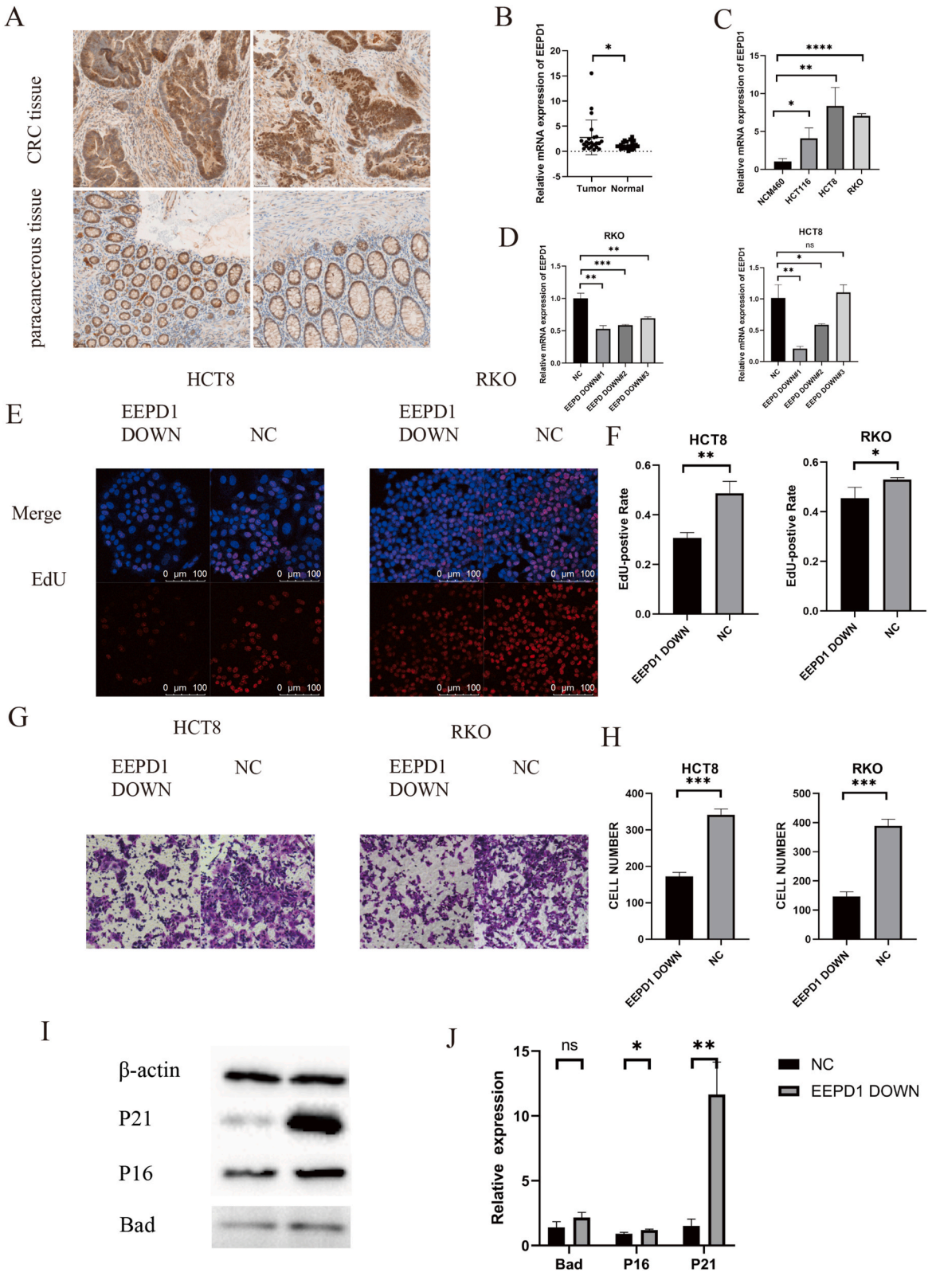

(caption on next page)

Fig. 11. EEPD1 promote cell proliferation and metastasis in CRC cells lines. (A) EEPD1 was significantly up-regulated in CRC tumor tissues According to immunohistochemistry (B) EEPD1 was significantly up-regulated in CRC tumor tissues According to RT-qPCR. (C) The expression of EEPD1 in CRC cell lines was higher than that in normal colorectal cell lines. (D)EEPD1 was knock down in HCT8 and RKO cell lines. (E, F) knockdown of EEPD1 significantly reduced the EdU-positive rate of EdU assay in RKO and HCT8 cells. (G, H) knockdown of EEPD1 significantly reduced the number of cells that cross the TRANSWELL chamber. (I, J) knockdown of EEPD1 significantly promoted the expression of P21 and P16 and showed an upward trend in the expression of Bad.

levels showed a positive association with infiltrating CD8 naive T cells, Mono-cytes, Neutrophils, and NKT cells in CRC. However, there was a negative correlation with infiltrating $CD8^+$ T, MAIT, iTreg, NK, Tc, Tex, Tfh, and Th1 cells (Fig. 6A and B).

TMB is an efficacy marker for immune checkpoint inhibitors with better immu-notherapy for a higher TMB effect [18]. MSI biomarkers can also predict the tumor immunotherapy effect [19]. The correlation between EEPD1, TMB, and MSI was ana-lyzed, revealing a significant correlation of EEPD1 with TMB in BLCA, COAD, STAD, THCA, THYM, UCS, and PRAD (Fig. 6C) and with MSI in COAD, STAD, UCS, LAML, PRAD and UVM (Fig. 6D). Especially, EEPD1 was negatively associated with TMB and MSI in COAD. Then, we analyzed the EEPD1 effect on PD-L1 inhibitors in the imvigor210 cohort. The results showed that tumors with a bad response to PD-L1 in-hibitors also possessed higher EEPD1 expression (Fig. 6E). Moreover, patients with higher EEPD1 expression showed a worse prognosis (Fig. 6F), depicting the sup-pressive role of EEPD1 in anti-PD-L1 immunotherapy.

Therefore, EEPD1 expression levels are correlated with immune cell infiltration, affecting immunotherapeutic efficacy.

3.6. EEPD1 and immune related genes

Afterward, co-expression analysis of the genes investigated the correlation be-tween EEPD1 and genes associated with immunity. The analyzed genes included im-mune checkpoints, chemokines, chemokines receptors, immune activation genes, im-munosuppressive genes, and MHC genes. In addition, the correlation between EEPD1 and tumor-related genes was also analyzed. This included EMT down and up, pyrop-tosis, autophagy, TGF-β1 signaling, Wnt/β-catenin signaling, ferroptosis, and MMR genes. Therefore, EEPD1 was negatively associated with almost all immune-related genes in COAD (Fig. 7A–F). Moreover, EEPD1 was positively correlated with most EMT down, pyroptosis, autophagy, TGF-β1 signaling, Wnt/β-catenin signaling, ferroptosis, and MMR genes in COAD (Fig. 8).

3.6.1. EEPD1 and drug resistance

The GDSC2 database helped analyze the correlation between EEPD1 and tumor resistance, with significantly increased tumor resistance to multiple drugs, including Docetaxel, Olaparib, Cyclophosphamide, Luminespib, OSI-027, RVX-208, AZD5991, ULK1_4989, AZD4547, Acetalax, Carmustine, Dactinomycin, MG-132, Buparlisib, GSK2578215A, UMI-77, Sepantronium bromide, BIBR-1532 and GSK591 (Fig. 9A–S). Moreover, EEPD1 made tumors more sensitive to other drugs, such as Axitinib, Palbo-ciclib, Oxaliplatin, Trametinib, Uprosertib, SCH772984, and Selumetinib (Fig. 9T–Z).

3.7. EEPD1 predicts prognosis in patients with colorectal cancer

CRC patients with high expression of EEPD1 in the TCGA database were screened out. We predicted the 1, 3, and 5 years OS using a nomogram depending on the EEPD1 expression, age, tumor stage, and T,N,M stages (Fig. 10A), then validating its predictive ability. According to the calibration plot, the nomogram predicted and actual survival showed a good correlation (Fig. 10B). The AUC value of the ROC curve for EEPD1 predicted OS was 0.713 (Fig. 10C). Moreover, the nomogram AUC values were 0.715, 0.642, and 0.657 with 1, 3, and 5 years of OS predictions, respectively (Fig. 10D). Therefore, the nomogram can predict the CRC patient prognosis with high EEPD1 expression.

3.8. EEPD1 promotes cell proliferation and migration in CRC

EEPD1 levels were substantially upregulated in tumors compared to normal tissues depending on IHC and RT-qPCR analysis of the collected CRC samples (Fig. 11A and B). In addition, EEPD1 expression was analyzed in various CRC cell lines by RT-qPCR. This indicated that the EEPD1 expression level in different CRC cell lines was higher than in normal colorectal cell line NCM460 (Fig. 11C). After that, three EEPD1 stRNAs were used to knock down the EEPD1 expression in RKO and HCT8 cells. The knockdown effect of stEEPD1#1 in both cell lines was confirmed using RT-qPCR (Fig. 11D). The EdU assay detected cell proliferation with a significantly reduced EdU-positive rate of RKO and HCT8 cells due to EEPD1 knockdown, indicating that silencing EEPD1 inhibits CRC cell proliferation (Fig. 11E and F). Moreover, EEPD1 can also affect the migration ability of CRC cells. Through transwell assay, it was observed that EEPD1 knockdown made it more challenging for the cell lines to cross the transwell chamber (Fig. 11G and H). Thus, silencing EEPD1 can inhibit the migration ability of CRC cells. Furthermore, based on our Western blot analysis of multiple cell cycle-related and apoptosis-related genes, EEPD1 knockdown resulted in a significant increase in the expression levels of P16 (CDKN2A, cyclin-dependent kinase inhibitor 2A) and P21 (CDKN1A, cyclin-dependent kinase inhibitor 1A) (Fig. 11 I, J). Besides, EEPD1 knockdown showed an upward trend in the expression of Bad (BCL2 associated agonist of cell death) (Fig. 11 I, J). This suggests that EEPD1 knockdown may exhibit an inhibitory effect on the cell cycle and a promotional effect on apoptosis.

In general, EEPD1 expression is significantly higher in tumors compared to normal tissues and shows elevated expression levels in

different CRC cell lines. Through the use of EEPD1 stRNAs to target and silence the EEPD1 gene, it was found that EEPD1 silencing can significantly inhibit the proliferation and migration abilities of CRC cells. Furthermore, EEPD1 silencing has inhibitory effects on cell cycle and a promotional effect on apoptosis. Overall, these results suggest that EEPD1 plays an important biological function in CRC and may be a potential therapeutic target.

4. Discussion

EEPD1 deficiency could be associated with the overall cancer process due to its role in DNA repair and genome stabilization [20]. There is limited research on its relationship with tumor and the expression and function of EEPD1 in cancer remain unclear. This study showed that EEPD1 was highly expressed in CHOL, COAD, DLBC, GBM, KICH, KIRC, KIRP, LAML, LIHC, PAAD, READ, and THYM cancers by analyzing TCGA and GTEx gene expression data. In contrast, EEPD1 expression was lower in BLCA, BRCA, CESC, ESCA, LUAD, LUSC, OV, PRAD, SKCM, TCGT, and THCA cancers than in normal tissues. One potential mechanism underlying the different prognostic value of EEPD1 in different cancers could be its interaction with specific signaling pathways or molecular networks that are dysregulated in a cancer type-specific manner. EEPD1 initiates HR by cleaving stressed replication forks, enabling cells to survive under sustained replication stress. However, EEPD1 cleaves replication forks to produce a lethal toxic intermediate for cells [12]. EEPD1 has complex effects on different tumors due to its ability to repair replication forks and maintain genome stability [20]. The expression levels of EEPD1 may be influenced by the tumor microenvironment, including interactions with immune cells, stromal cells, and the extracellular matrix. The presence of specific immune cell subtypes or stromal components in the tumor microenvironment could impact the prognostic value of EEPD1 by altering its functional role in promoting or suppressing cancer progression. Besides, genetic alterations or epigenetic modifications in the EEPD1 may contribute to its differential prognostic value across different cancer types.

EEPD1 is highly expressed in CRC. Clinical data analysis also revealed that EEPD1 expression in advanced CRC is usually higher than in early CRC. Moreover, the prognosis of patients with elevated EEPD1 levels is worse than those having low EEPD1 levels. Therefore, EEPD1 may behave as an oncogene and become an important biomarker indicating CRC prognosis. Consequently, a nomogram was established based on EEPD1 and several clinical parameters to predict the OS of CRC patients. Calibration plots and ROC curve validations indicated the good predictive ability of EEPD1. This nomogram can enable clinicians to make decisions regarding the prognosis of patients and subsequent treatment.

GSVA showed that EEPD1 is primarily associated with the Wnt/β-catenin signaling pathway. It is crucial in animal embryonic development and organ formation [21]. This signaling has been widely associated with various tumors [22]. Moreover, WNT hyperactivation due to mutations in adenomatous polyposis coli (APC) is a CRC hallmark [23]. Mutations in β-catenin were frequently observed in CRC [24] and related to MSI [25]. GSEA based on GO, KEGG, and Reactome databases also revealed that EEPD1 was closely associated with RNA processing, ribosome, and protein translation, suggesting its crucial role in tumor development. In the subsequent gene co-expression analysis, EEPD1 was positively correlated with most genes in TGF-β1 signaling, Wnt/β-catenin signaling, and MMR. TGF-β1 controls multiple life processes [26] and is associated with tumor proliferation and EMT [27]. In addition, the immunotherapy effect with PD-L1 inhibitors can be elevated by inhibiting TGF-β1 [28]. MMR gene mutations can cause MSI in CRC and are related to immune checkpoint inhibitor efficacy [29]. Moreover, CRC cells extensively proliferate and migrate due to EEPD1, even though the exact mechanism remains unknown.

TME has been a hot topic in tumors, where immune cell infiltration significantly affects tumor development [30,31]. $CD8^+$ T, MAIT, and NK cells play crucial roles in anti-tumor immune responses, especially $CD8^+$ T cells which have a key role in eliminating tumor cells [32–35]. EEPD1 shows a negative correlation with these cells, suggesting a negative regulatory role in inhibiting the infiltration and activation of these immune cell types. This negative regulatory effect may lead to an immunosuppressive state in the tumor immune microenvironment, aiding in the evasion of immune surveillance and tumor development. Then, gene co-expression analysis indicated that EEPD1 was negatively correlated with most immune-related genes, such as immune checkpoints, chemokines, chemokines receptors, and immune activation genes. Thus, EEPD1 can suppress the immune system response to tumors in multiple ways. The correlation between EEPD1 and TMB and MSI also suggests its important role in tumor immune therapy. High TMB and MSI are usually associated with better immune treatment outcomes, and the negative correlation between EEPD1 and TMB and MSI may affect the sensitivity of tumors to immune therapy, consistent with our previous results. In addition, the association between EEPD1 and the efficacy of PD-L1 inhibitors and patient prognosis further highlights its important role in anti-PD-L1 immunotherapy. Elevated expression of EEPD1 may be correlated with poor anti-tumor effects of PD-L1 inhibitors and worse patient prognosis, suggesting that EEPD1 could be a potential immunotherapy target. Taken together, the complex regulatory role of EEPD1 in tumor immunity suggests that it may be an important regulatory factor that influences the balance of the tumor immune microenvironment and the sensitivity of tumors to immune therapy. Further research will help to elucidate the specific mechanisms of EEPD1 in tumor immune regulation and provide an important theoretical basis for developing new immunotherapy strategies.

Although our research has made some progress, there are also some notable limitations that need to be addressed. Firstly, the number of tissue samples collected in our experiments was not sufficient, which may affect the reliability and generalizability of the results. Secondly, while we have drawn some important conclusions from the bioinformatics analysis, these conclusions still require further experimental validation for confirmation and support. Therefore, we honestly acknowledge that addressing these limitations will require continued support and effort in future research.

In conclusion, we performed the first pan-cancer analysis of EEPD1 and observed that EEPD1 was abnormally expressed in cancers. EEPD1 was associated with prognosis, TME, immune cell infiltration, TMB, MSI, immune modulation, multiple tumor-related signaling pathways, and drug resistance across various human cancers. Especially bioinformatic analysis and experimental confirmation

revealed that EEPD1 was upregulated across numerous samples, predicting a poor CRC prognosis. Then, a nomogram helped determine the OS of CRC patients depending on EEPD1 expression and several clinical parameters. Furthermore, EEPD1 enhances the infiltration of CD8 naive T cells, monocytes, Neutrophils, and NKT cells, while inhibiting the infiltration of $CD8^+$ T, MAIT, iTreg, NK, Tc, Tex, Tfh, and Th1 cells. Besides, EEPD1 is related to TGF-β1 and Wnt/β-catenin signaling. Moreover, EEPD1 knockdown suppressed CRC cell proliferation and migration ， and has complex effects on cell cycle. Therefore, the multi-functional roles of EEPD1 in pan-cancer and its oncogenic role in CRC could be a theoretical basis for precision therapy in human cancers.

Ethics statement

The study involving human participants was reviewed and approved by the Ethics Committee of Zhejiang Provincial People's Hospital on April 1, 2024 (ZPPHEC 2024O (079)). Patients/participants provided written informed consent for their participation in this study.

Funding

This project was supported by the Natural Science Foundation of Zhejiang Province (LQ21H160042).

Data availability statement

Data will be made available on request.

CRediT authorship contribution statement

Yang Guo: Writing – original draft, Validation, Methodology, Formal analysis, Conceptualization. **Shujin Li:** Writing – original draft, Methodology, Formal analysis, Conceptualization. **Zhan Shi:** Writing – original draft, Validation. **Bingchen Chen:** Software. **Ziang Wan:** Data curation. **Peng Yu:** Software. **Boan Zheng:** Methodology. **Wenjing Gong:** Formal analysis. **Rui Chai:** Investigation. **Shiliang Tu:** Writing – review & editing, Data curation. **Hang Yuan:** Writing – review & editing, Formal analysis, Conceptualization.

Declaration of competing interest

The authors declare that they have no known competing financial interests or personal relationships that could have appeared to influence the work reported in this paper.

Appendix A. Supplementary data

Supplementary data to this article can be found online at https://doi.org/10.1016/j.heliyon.2024.e29285.

References

[1] H. Sung, J. Ferlay, R.L. Siegel, M. Laversanne, I. Soerjomataram, A. Jemal, F. Bray, Global cancer statistics 2020: GLOBOCAN estimates of incidence and mortality worldwide for 36 cancers in 185 countries, CA A Cancer J. Clin. 71 (3) (2021) 209–249.
[2] L.H. Biller, D. Schrag, Diagnosis and treatment of metastatic colorectal cancer: a review, JAMA 325 (7) (2021) 669–685, https://doi.org/10.1001/jama.2021.0106.
[3] M.K. Zeman, K.A. Cimprich, Causes and consequences of replication stress, Nat. Cell Biol. 16 (1) (2014) 2–9, https://doi.org/10.1038/ncb2897.
[4] S. Saxena, L. Zou, Hallmarks of DNA replication stress, Mol. Cell 82 (12) (2022) 2298–2314, https://doi.org/10.1016/j.molcel.2022.05.004.
[5] A. Maréchal, L. Zou, DNA damage sensing by the ATM and ATR kinases, Cold Spring Harbor Perspect. Biol. 5 (9) (2013) a012716, https://doi.org/10.1101/cshperspect.a012716.
[6] A. Costes, S.A. Lambert, Homologous recombination as a replication fork escort: fork-protection and recovery, Biomolecules 3 (1) (2012) 39–71, https://doi.org/10.3390/biom3010039.
[7] Saada A. Ait, S.A.E. Lambert, A.M. Carr, Preserving replication fork integrity and competence via the homologous recombination pathway, DNA Repair 71 (2018) 135–147, https://doi.org/10.1016/j.dnarep.2018.08.017.
[8] H.S. Kim, J.A. Nickoloff, Y. Wu, E.A. Williamson, G.S. Sidhu, B.L. Reinert, A.S. Jaiswal, G. Srinivasan, B. Patel, K. Kong, S. Burma, S.H. Lee, R.A. Hromas, Endonuclease EEPD1 is a gatekeeper for repair of stressed replication forks, J. Biol. Chem. 292 (7) (2017) 2795–2804, https://doi.org/10.1074/jbc.M116.758235.
[9] Y. Wu, S.H. Lee, E.A. Williamson, B.L. Reinert, J.H. Cho, F. Xia, A.S. Jaiswal, G. Srinivasan, B. Patel, A. Brantley, D. Zhou, L. Shao, R. Pathak, M. Hauer-Jensen, S. Singh, K. Kong, X. Wu, H.S. Kim, T. Beissbarth, J. Gaedcke, S. Burma, J.A. Nickoloff, R.A. Hromas, EEPD1 rescues stressed replication forks and maintains genome stability by promoting end resection and homologous recombination repair, PLoS Genet. 11 (12) (2015) e1005675, https://doi.org/10.1371/journal.pgen.1005675.
[10] A. Bowry, R.D.W. Kelly, E. Petermann, Hypertranscription and replication stress in cancer, Trends Cancer 7 (9) (2021) 863–877, https://doi.org/10.1016/j.trecan.2021.04.006.
[11] M.K. Zeman, K.A. Cimprich, Causes and consequences of replication stress, Nat. Cell Biol. 16 (1) (2014) 2–9, https://doi.org/10.1038/ncb2897.
[12] R. Hromas, H.S. Kim, G. Sidhu, E. Williamson, A. Jaiswal, T.A. Totterdale, J. Nole, S.H. Lee, J.A. Nickoloff, K.Y. Kong, The endonuclease EEPD1 mediates synthetic lethality in RAD52-depleted BRCA1 mutant breast cancer cells, Breast Cancer Res. 19 (1) (2017) 122, https://doi.org/10.1186/s13058-017-0912-8. PMID: 29145865; PMCID: PMC5693420.

[13] R. Bonneville, M.A. Krook, E.A. Kautto, J. Miya, M.R. Wing, H.Z. Chen, J.W. Reeser, L. Yu, S. Roychowdhury, Landscape of microsatellite instability across 39 cancer types, JCO Precis Oncol. 2017 (2017), https://doi.org/10.1200/PO.17.00073, 17.00073.
[14] D.C. Hinshaw, L.A. Shevde, The tumor microenvironment innately modulates cancer progression, Cancer Res. 79 (18) (2019 Sep 15) 4557–4566, https://doi.org/10.1158/0008-5472.CAN-18-3962.
[15] J. Wu, L. Li, H. Zhang, Y. Zhao, H. Zhang, S. Wu, B. Xu, A risk model developed based on tumor microenvironment predicts overall survival and associates with tumor immunity of patients with lung adenocarcinoma, Oncogene 40 (26) (2021) 4413–4424, https://doi.org/10.1038/s41388-021-01853-y.
[16] D. Liu, X. Yang, X. Wu, Tumor immune microenvironment characterization identifies prognosis and immunotherapy-related gene signatures in melanoma, Front. Immunol. 12 (2021) 663495, https://doi.org/10.3389/fimmu.2021.663495.
[17] Z. Zhang, W.R. Karthaus, Y.S. Lee, V.R. Gao, C. Wu, J.W. Russo, M. Liu, J.M. Mota, W. Abida, E. Linton, E. Lee, S.D. Barnes, H.A. Chen, N. Mao, J. Wongvipat, D. Choi, X. Chen, H. Zhao, K. Manova-Todorova, E. de Stanchina, M.E. Taplin, S.P. Balk, D.E. Rathkopf, A. Gopalan, B.S. Carver, P. Mu, X. Jiang, P.A. Watson, C. L. Sawyers, Tumor microenvironment-derived NRG1 promotes antiandrogen resistance in prostate cancer, Cancer Cell 38 (2) (2020) 279–296.e9, https://doi.org/10.1016/j.ccell.2020.06.005.
[18] R.M. Samstein, C.H. Lee, A.N. Shoushtari, M.D. Hellmann, R. Shen, Y.Y. Janjigian, D.A. Barron, A. Zehir, E.J. Jordan, A. Omuro, T.J. Kaley, S.M. Kendall, R. J. Motzer, A.A. Hakimi, M.H. Voss, P. Russo, J. Rosenberg, G. Iyer, B.H. Bochner, D.F. Bajorin, H.A. Al-Ahmadie, J.E. Chaft, C.M. Rudin, G.J. Riely, S. Baxi, A. L. Ho, R.J. Wong, D.G. Pfister, J.D. Wolchok, C.A. Barker, P.H. Gutin, C.W. Brennan, V. Tabar, I.K. Mellinghoff, L.M. DeAngelis, C.E. Ariyan, N. Lee, W.D. Tap, M.M. Gounder, S.P. D'Angelo, L. Saltz, Z.K. Stadler, H.I. Scher, J. Baselga, P. Razavi, C.A. Klebanoff, R. Yaeger, N.H. Segal, G.Y. Ku, R.P. DeMatteo, M. Ladanyi, N.A. Rizvi, M.F. Berger, N. Riaz, D.B. Solit, T.A. Chan, L.G.T. Morris, Tumor mutational load predicts survival after immunotherapy across multiple cancer types, Nat. Genet. 51 (2) (2019) 202–206, https://doi.org/10.1038/s41588-018-0312-8.
[19] K. Ganesh, Z.K. Stadler, A. Cercek, R.B. Mendelsohn, J. Shia, N.H. Segal, L.A. Diaz Jr., Immunotherapy in colorectal cancer: rationale, challenges and potential, Nat. Rev. Gastroenterol. Hepatol. 16 (6) (2019) 361–375, https://doi.org/10.1038/s41575-019-0126-x.
[20] J.A. Nickoloff, N. Sharma, L. Taylor, S.J. Allen, S.H. Lee, R. Hromas, Metnase and EEPD1: DNA repair functions and potential targets in cancer therapy, Front. Oncol. 12 (2022) 808757, https://doi.org/10.3389/fonc.2022.808757. PMID: 35155245; PMCID: PMC8831698.
[21] J. Liu, Q. Xiao, J. Xiao, C. Niu, Y. Li, X. Zhang, Z. Zhou, G. Shu, G. Yin, Wnt/β-catenin signalling: function, biological mechanisms, and therapeutic opportunities, Signal Transduct. Targeted Ther. 7 (1) (2022) 3, https://doi.org/10.1038/s41392-021-00762-6.
[22] F. Yu, C. Yu, F. Li, Y. Zuo, Y. Wang, L. Yao, C. Wu, C. Wang, L. Ye, Wnt/β-catenin signaling in cancers and targeted therapies, Signal Transduct. Targeted Ther. 6 (1) (2021) 307, https://doi.org/10.1038/s41392-021-00701-5.
[23] E.M. Schatoff, S. Goswami, M.P. Zafra, M. Foronda, M. Shusterman, B.I. Leach, A. Katti, B.J. Diaz, L.E. Dow, Distinct colorectal cancer-associated APC mutations dictate response to tankyrase inhibition, Cancer Discov. 9 (10) (2019) 1358–1371, https://doi.org/10.1158/2159-8290.CD-19-0289.
[24] V. Johnson, E. Volikos, S.E. Halford, Sadat Eftekhar Et, S. Popat, I. Talbot, K. Truninger, J. Martin, J. Jass, R. Houlston, W. Atkin, I.P. Tomlinson, A.R. Silver, Exon 3 beta-catenin mutations are specifically associated with colorectal carcinomas in hereditary non-polyposis colorectal cancer syndrome, Gut 54 (2) (2005) 264–267, https://doi.org/10.1136/gut.2004.048132.
[25] K. Shitoh, T. Furukawa, M. Kojima, F. Konishi, M. Miyaki, T. Tsukamoto, H. Nagai, Frequent activation of the beta-catenin-Tcf signaling pathway in nonfamilial colorectal carcinomas with microsatellite instability, Genes Chromosomes Cancer 30 (1) (2001) 32–37, https://doi.org/10.1002/1098-2264(2000)9999:9999<::aid-gcc1065>3.0.co;2-i.
[26] G. de Streel, S. Lucas, Targeting immunosuppression by TGF-β1 for cancer immunotherapy, Biochem. Pharmacol. 192 (2021) 114697, https://doi.org/10.1016/j.bcp.2021.114697.
[27] Q. Xue, H. Jiang, J. Wang, D. Wei, LASP1 induces epithelial-mesenchymal transition in lung cancer through the TGF-β1/smad/snail pathway, Cancer Res. J. 2021 (2021) 5277409, https://doi.org/10.1155/2021/5277409.
[28] N.P. Tschernia, J.L. Gulley, Tumor in the crossfire: inhibiting TGF-β to enhance cancer immunotherapy, BioDrugs 36 (2) (2022) 153–180, https://doi.org/10.1007/s40259-022-00521-1. Epub 2022 Mar 30.
[29] I.H. Sahin, M. Akce, O. Alese, W. Shaib, G.B. Lesinski, B. El-Rayes, C. Wu, Immune checkpoint inhibitors for the treatment of MSI-H/MMR-D colorectal cancer and a perspective on resistance mechanisms, Br. J. Cancer 121 (10) (2019) 809–818, https://doi.org/10.1038/s41416-019-0599-y.
[30] T.F. Gajewski, H. Schreiber, Y.X. Fu, Innate and adaptive immune cells in the tumor microenvironment, Nat. Immunol. 14 (10) (2013) 1014–1022, https://doi.org/10.1038/ni.2703.
[31] X. Mao, J. Xu, W. Wang, C. Liang, J. Hua, J. Liu, B. Zhang, Q. Meng, X. Yu, S. Shi, Crosstalk between cancer-associated fibroblasts and immune cells in the tumor microenvironment: new findings and future perspectives, Mol. Cancer 20 (1) (2021) 131, https://doi.org/10.1186/s12943-021-01428-1.
[32] S. Shang, Y.W. Yang, F. Chen, L. Yu, S.H. Shen, K. Li, B. Cui, X.X. Lv, C. Zhang, C. Yang, J. Liu, J.J. Yu, X.W. Zhang, P.P. Li, S.T. Zhu, H.Z. Zhang, F. Hua, TRIB3 reduces CD8+ T cell infiltration and induces immune evasion by repressing the STAT1-CXCL10 axis in colorectal cancer, Sci. Transl. Med. 14 (626) (2022) eabf0992, https://doi.org/10.1126/scitranslmed.abf0992.
[33] Q. Lou, R. Liu, X. Yang, W. Li, L. Huang, L. Wei, H. Tan, N. Xiang, K. Chan, J. Chen, H. Liu, miR-448 targets Ido1 and regulates CD8+ T cell response in human colon cancer, J. Immunother. Cancer 7 (1) (2019) 210, https://doi.org/10.1186/s40425-019-0691-0.
[34] L. Ling, Y. Lin, W. Zheng, S. Hong, X. Tang, P. Zhao, M. Li, J. Ni, C. Li, L. Wang, Y. Jiang, Circulating and tumor-infiltrating mucosal associated invariant T (MAIT) cells in colorectal cancer patients, Sci. Rep. 6 (2016) 20358, https://doi.org/10.1038/srep20358.
[35] O. Melaiu, V. Lucarini, L. Cifaldi, D. Fruci, Influence of the tumor microenvironment on NK cell function in solid tumors, Front. Immunol. 10 (2020) 3038, https://doi.org/10.3389/fimmu.2019.03038.